Design and Optimization of Liquid Crystal RIS-Based Visible Light Communication Receivers

Sylvester Aboagye, *Member, IEEE*, Alain R. Ndjiongue, Telex M. N. Ngatched, *Senior Member, IEEE*, and Octavia A. Dobre, *Fellow, IEEE*

***Abstract*—In the design of reconfigurable intelligent surfaces (RISs)-aided visible light communication (VLC) systems, most studies have focused on the deployment of mirror arrays and metasurfaces on walls to influence signal propagation and enhance communication performance. This paper provides a new research direction in the design and performance optimization of RIS-aided VLC systems whereby voltage-controlled tunable liquid crystals (LCs) are deployed as part of the VLC receiver. The purpose of the LC RIS is to provide incident light steering and intensity amplification in order to improve the received signal strength and the corresponding achievable data rate. More specifically, an LC RIS-based VLC receiver design is proposed and its operating principles and the channel model for a VLC system with such a receiver are provided. Since the refractive index of the LC RIS plays a critical role in the wave-guiding and light amplification capabilities of this novel receiver, a rate maximization problem is considered to achieve the optimal refractive index and the required voltage to obtain the best light amplification and data rate performances. This communication design problem is a non-convex optimization problem for which a metaheuristic approach is developed based on the sine-cosine algorithm. Simulation results are used to confirm the considerable data rate improvement by the proposed LC RIS-based VLC receiver and optimization algorithm when compared to a VLC receiver without the LC RIS and a baseline scheme, respectively.**

***Index Terms*—Reconfigurable intelligent surface, visible light communication, liquid crystals, light amplification, metaheuristic.**

I. Introduction

VISIBLE light communication (VLC) has emerged as a disruptive technology that promises low-cost implementation, huge unlicensed bandwidth and high data rate to complement radio frequency-based communication systems. VLC has sparked the interest of the research community and the industry in recent years and is envisioned as a key evolutionary technology to enable ultrahigh data rate (potentially up to 100 Gb/s) in beyond fifth generation systems [1]. Inspired by the promising advantages of VLC, significant research efforts have been devoted to its design and performance analysis and can be categorized into areas such as network architecture design, user mobility, transmitter and receiver designs, access point (AP) assignment and resource allocation, interference management, and reconfigurable intelligent surfaces (RISs)-aided design [2], [3], [4]. Although the aforementioned areas are equally important in enhancing the performance gain of VLC systems, there has been few studies on the design and performance analysis of VLC receivers with light steering and amplification capabilities that can significantly improve the received signal-to-noise ratio. That is the focus of this paper.

A typical VLC receiver (i.e., ordinary VLC receiver) is composed of a convex lens and a photodetector (PD) characterized by a small physical area, A_{PD}, and a field-of-view (FoV). In VLC, the incoming light from the source must fall within the FoV of the PD in order to successfully recover the transmitted data. To achieve that, ordinary VLC receivers use convex lens as etendue reducers to collect and focus the incoming light onto the PD. However, as discussed in [5], the use of a convex lens can result in up to 30% losses in the incident light power due to reflection at the len's upper surface. Moreover, convex lenses cannot dynamically steer the impinging light beam and, as a result, can limit the detection capabilities of the receiver, especially when the angle of incidence is large. As examined in [6], methods such as (i) extending a flexible matrix with dielectric nano-resonators, (ii) modifying the phase of an amorphous crystalline transition in a chalcogenide, and (iii) ultra-fast switching of mie-resonant silicon nano-structure, are among the various ways of steering incoming beam. However, such methods typically weakly affect the refracted beam, even at high optical intensity.

Motivated by the numerous appealing functionalities and low cost of RISs, the idea of using liquid crystal (LC) as an RIS to overcome this specific drawback and amplify the incident light power, without using power amplifiers, has recently been proposed in [5], [6]. The LC RIS has electronically tunable physico-chemical properties (e.g., the refractive index) that can be controlled by re-orienting the LC molecules via an external electrical field. By tunning the physico-chemical properties, the LC RIS can steer any incident light beam such that the refracted beam falls within the FoV of the PD. However, the realization of such an LC RIS-based VLC receiver is still far from practice as there has been limited research on it. In [7], [8], [9], [10], the authors demonstrated the use of LCs as dynamic optical filters for ambient light and interference suppression in different VLC and visible light positioning scenarios. This paper, for the first time, proposes a practical design for LC RIS-based VLC receivers with light steering and amplification capabilities, and

Manuscript received 28 July 2022; revised 17 September 2022; accepted 30 September 2022. Date of publication 4 October 2022; date of current version 11 October 2022. This work was supported in part by the Natural Science and Engineering Research Council of Canada (NSERC) through its Discovery Program, in part by Memorial University VPR Program, and in part by Ocean Frontier Institute. *(Corresponding author: Telex M. N. Ngatched.)*

The authors are with the Department of Electrical and Computer Engineering, Memorial University, St. John's, NL A1C5S7, Canada (e-mail: sbaboagye@mun.ca; arndjiongue@mun.ca; tngatched@grenfell.mun.ca; odobre@mun.ca).

Digital Object Identifier 10.1109/JPHOT.2022.3211730

a framework to optimize its communication performance. The main contributions are summarized as follows:

- A novel LC RIS-based receiver technology is proposed to enhance the received signal strength and the corresponding achievable rate in VLC systems.
- A channel model for the LC RIS-based receiver is proposed and the equation characterizing the achievable rate is derived. In addition, mathematical expressions for the incident light amplification are provided.
- A framework to optimize the performance of the new LC RIS-based receiver is presented. To the best of the authors' knowledge, this is the first channel modelling and optimization framework for an LC RIS-based receiver.
- Simulation results are presented to demonstrate the significant performance gains of the LC RIS-based receiver and the proposed optimization algorithm, respectively, when compared with an ordinary receiver and a benchmark scheme (BSch).

The rest of the paper is organized as follows. Section II describes the system and channel models for a VLC system with an LC RIS-based receiver. Section III formulates the data rate optimization problem and proposes a solution to tune the refractive index of the LC RIS to yield the optimal data rate performance. In Section IV, simulation results are reported and final conclusions are drawn in Section V.

II. System and Channel Model

This section describes the indoor VLC environment and details the structure of the LC RIS-based receiver and its channel model. Finally, the principle of incident light amplification for this receiver is presented and the expression for the amplification coefficient is derived.

A. LC RIS-Based Receiver

We consider the downlink of an indoor VLC system composed of a VLC-enabled ceiling light emitting diode array (i.e., a VLC AP) and a user equipped with a nematic LC RIS-based VLC receiver as depicted in Fig. 1(a). In this figure, the LC RIS-based receiver differs from an ordinary VLC receiver, which is typically composed of an optical filter, optical concentrator, and a PD by having an LC RIS module placed right in front of the PD. Similar to the LC RIS module structure in [5], [6], it is composed of tin oxide nanodisks with LC infiltration (i.e., the LC cell) sandwiched by different layers of thin materials. These layers are the anti-reflection polarizer for filtering any incoming light, a glass substrate for generating the preferred direction of orientation for the LC molecules, indium tin oxide to assist with heat production and control, and a photoalignment film for guiding light beam through the LC cell.

Fig. 1(b) describes the geometry of light propagation inside the LC cell when an external voltage, v_{e}, which is greater than the threshold voltage, v_{th}, is applied. In this figure, the emitted optical signal from the AP, denoted as L_1, travels through the air medium (i.e., the VLC channel) with a refractive index η_a and incidents on the interface between air and LC cell at an angle φ. Since no light is absorbed at this interface, part of the optical signal L_1 gets reflected while the remaining signal, L_2, undergoes refraction, at an angle θ, as it propagates through the LC cell with thickness d and refractive index η_c. The propagation characteristics (e.g., direction and intensity) of the optical signal as it travels through and exits the LC cell can be controlled through an eletric field-induced molecular reorientation which, in turn, causes changes in the refractive index η_c. Thus, the refractive index is the main parameter that offers the LC RIS its wave-guiding capability.

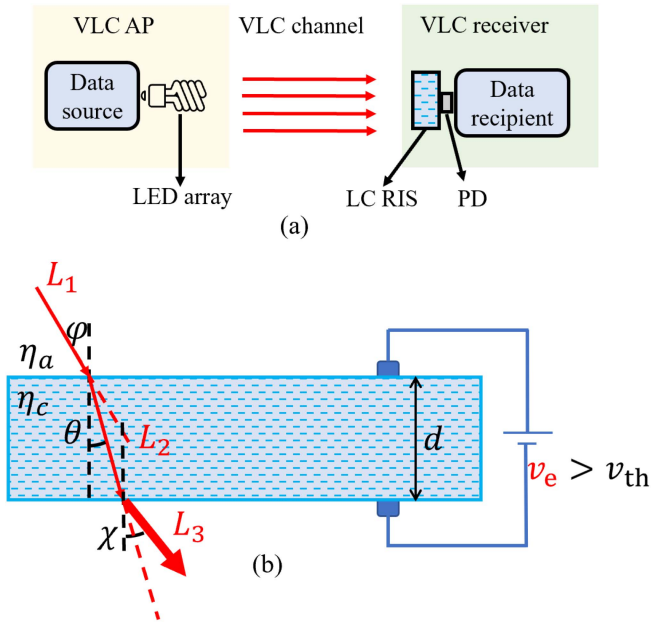

Fig. 1. VLC system model with LC RIS-based receiver: (a) VLC transmission system with a single AP and LC RIS-based receiver; (b) Geometry of optical signal propagation through the LC cell.

B. Channel Model

The channel model for the line-of-sight (LoS) communication in the system model in Fig. 1(a) can be described by the signal propagation through air and the LC cell, with the former represented by the direct current (DC) gain and the latter by the transition coefficient. Mathematically, it can be given as

$$H = G_{\mathrm{LoS}} \times \alpha_{\mathrm{LC}}, \tag{1}$$

where H is the channel gain between the AP and the receiver, G_{LoS} represents the DC gain of the LoS link between the AP and the LC RIS module, and α_{LC} denotes the transition coefficient. The LoS channel gain can be expressed as

$$G_{\mathrm{LoS}} = \frac{A_{\mathrm{PD}}\,(m+1)}{2\pi l^2}\cos^m(\Phi)\,T(\varphi)\,G(\varphi), \tag{2}$$

where A_{PD} is the area of the PD, $m = -\log_2(\cos(\phi_{1/2}))^{-1}$, is the Lambertian emission order with $\phi_{1/2}$ being the LED's semi–angle at half power, l is the distance between the AP and the receiver, Φ represents the angle of irradiance, φ is the angle of incidence, $T(\varphi)$ is the gain of the receiver's optical filter, $G(\varphi) = \frac{f^2}{\sin^2\varphi}, 0 \le \varphi \le \varphi_{\mathrm{FoV}}$, is the gain of the non-imaging

concentrator with an internal refractive index f. $\varphi_{\mathrm{FoV}} \leq \frac{\pi}{2}$ is the FoV of the PD.

The transition coefficient quantifies the impact that the LC RIS module has on the overall channel gain. This coefficient can be obtained by analysing the propagation of light as it enters the LC RIS, travels through the LC cell and exits it. Assuming an un-polarized incident light, the angular reflectance – specifying the amount of any incident light I_i that gets reflected by the LC RIS – can be determined according to the Fresnel's equation [11]

$$R_{\mathrm{ac}}(\varphi,\theta) = \frac{1}{2}\left(\frac{\eta\cos\varphi - \cos\theta}{\eta\cos\varphi + \cos\theta}\right)^2 + \frac{1}{2}\left(\frac{\cos\varphi - \eta\cos\theta}{\cos\varphi + \eta\cos\theta}\right)^2, \tag{3}$$

where $\eta = \eta_{\mathrm{c}}/\eta_{\mathrm{a}}$ is the relative refractive index, and R_{ac} is the angular reflectance at the LC RIS. By using the Snell's law, $\eta_{\mathrm{a}}\sin\varphi = \eta_{\mathrm{c}}\sin\theta$, the angular reflectance can be given as a function of the angle of incidence φ as

$$R_{\mathrm{ac}}(\varphi) = \frac{1}{2}\left(\frac{\eta^2\cos\varphi - \sqrt{\eta^2 - \sin^2\varphi}}{\eta^2\cos\varphi + \sqrt{\eta^2 - \sin^2\varphi}}\right)^2 + \frac{1}{2}\left(\frac{\cos\varphi - \sqrt{\eta^2 - \sin^2\varphi}}{\cos\varphi + \sqrt{\eta^2 - \sin^2\varphi}}\right)^2. \tag{4}$$

Since no light is absorbed at the interface between air and the LC RIS, the angular transmittance, T_{ac}, representing the amount of the incident light that is being refracted through the LC RIS can be given as $T_{\mathrm{ac}}(\varphi) = 1 - R_{\mathrm{ac}}(\varphi)$ and the resulting refracted radiance that propagates through the LC cell is

$$I_r = (\eta)^2 T_{\mathrm{ac}}(\varphi) I_i. \tag{5}$$

As the light signal exits the LC RIS, it gets attenuated by the angular reflectance

$$R_{\mathrm{ca}}(\theta) = \frac{1}{2}\left(\frac{\eta_1^2\cos\theta - \sqrt{\eta_1^2 - \sin^2\theta}}{\eta_1^2\cos\theta + \sqrt{\eta_1^2 - \sin^2\theta}}\right)^2 + \frac{1}{2}\left(\frac{\cos\theta - \sqrt{\eta_1^2 - \sin^2\theta}}{\cos\theta + \sqrt{\eta_1^2 - \sin^2\theta}}\right)^2, \tag{6}$$

where $\eta_1 = \eta_{\mathrm{a}}/\eta_{\mathrm{c}}$ and corresponding angular transmittance T_{ca} can be obtained as $T_{\mathrm{ca}}(\varphi) = 1 - R_{\mathrm{ca}}(\varphi)$. The refracted radiance that is detected by the PD can therefore be given as

$$I_e = (\eta_1)^2 T_{\mathrm{ca}}(\theta) I_r. \tag{7}$$

By substituting (5) in (7),

$$I_e = (\eta_1)^2 T_{\mathrm{ca}}(\theta) \times (\eta)^2 T_{\mathrm{ac}}(\varphi) I_i, \tag{8}$$

from which the transition coefficient α_{LC} can be obtained as

$$\alpha_{\mathrm{LC}} = T_{\mathrm{ca}}(\varphi) \times T_{\mathrm{ac}}(\theta). \tag{9}$$

It can be observed from (9) that the transition coefficient can be optimized by tunning the refractive index η_c of the LC RIS. Tunning η_c involves varying the tilt angle ξ that specifies the molecular orientation of the LC cell. The relationship between the refractive index and the tilt angle can be expressed as [12]

$$\frac{1}{\eta_{\mathrm{c}}^2(\xi)} = \frac{\cos^2\xi}{\eta_{\mathrm{e}}^2} + \frac{\sin^2\xi}{\eta_{\mathrm{o}}^2}, \tag{10}$$

where $\eta_{\mathrm{c}}(\xi)$ is the refractive index of the LC for the given tilt angle ξ, and η_{e} and η_{o} are the extraordinary and ordinary refractive indices of the LC. However, the tilt angle is controlled by an externally applied voltage and this relationship can be characterized by

$$\xi = \begin{cases} 0, & v_e \leq v_{th} \\ \frac{\pi}{2} - 2\tan^{-1}\left[\exp\left(-\frac{v_e - v_{th}}{v_0}\right)\right], & v_e > v_{th}, \end{cases} \tag{11}$$

where v_e is the externally applied voltage, v_{th} is a critical voltage at which the tilting process begins, and v_0 is a constant. Since ξ is controlled by the voltage applied to the LC cell in accordance with (11), the LC cell can be readily used as a voltage controlled RIS that can manipulate the propagation of light by adjusting its refractive index and the refraction angle to steer the incident light beam.

C. Amplification Gain Coefficient

This subsection details how the LC RIS module can be used to provide light amplification and enhance signal reception as depicted in Fig. 1(b). It can be observed from this figure that the intensity of the light emerging from the LC module at the refraction angle χ, labelled L_3, is greater than the intensity of the incident light, L_1. This light amplification occurs as a result of stimulated emission where incident photons interact with LC's molecules excited by an external voltage causing them to drop to a lower energy level to create new photons that are coherent. When an optical signal of intensity L_1 travels through an LC cell of depth d that has undergone population inversion, the intensity of the output beam L_3 can be given by the Beer's absorption law [13], however, with a negative absorption coefficient Γ as given in (12). In this equation, Γ denotes the amplification gain coefficient and the term $\exp(\Gamma d)$ represents the 'e-fold' increase of the intensity of the incident light.

$$L_3 = L_1 \times \exp(\Gamma d) \times \alpha_{\mathrm{LC}}. \tag{12}$$

According to the dynamic two-wave coupling theory, the amplification gain coefficient can be expressed as [14], [15]

$$\Gamma = \frac{2\pi\eta_c^3}{\lambda\cos\varphi} r_{\mathrm{eff}} E, \tag{13}$$

where λ is the wavelength of the transmitted light, r_{eff} is the electro-optic coefficient, and E [V/m] is the externally applied electric field. It can be observed from (13) that the wavelength of the light beam, the refractive index of the LC RIS, and the applied voltage affect the amplification gain of the LC RIS. To that end, those values must be carefully selected to ensure optimum performance.

III. Achievable Rate Optimization

A. Rate Maximization Problem

The achievable rate of the RIS-aided VLC system in Fig. 1(a) is given by the lower bound on the channel capacity [16]

$$R^{\mathrm{LC}} = B\log_2\left(1+\frac{\exp(1)}{2\pi}\frac{\left((P/q)\exp\left(\Gamma d\right)R_{\mathrm{PD}}H\right)^2}{N_oB}\right), \tag{14}$$

where B, P, q, R_{PD}, and N_o denote the information carrying bandwidth, the optical power, the ratio of the transmitted optical power to the electrical power, the responsivity of the PD, and the power spectral density of noise, respectively. This paper proposes to optimize (14) by intelligently controlling the refractive index, η_{c}, of the LC cell. For the optimal refractive index η_{c}^*, the required tilt angle of the LC molecules and the corresponding external voltage can be determined from (10) and (11), respectively. This data rate optimization design problem can be formulated as

$$\begin{aligned}&\max_{\eta_{\mathrm{c}}} R^{\mathrm{LC}}\\ &\text{s.t.}\\ &C1: 1.5 \le \eta_{\mathrm{c}} \le 1.7,\end{aligned} \tag{15}$$

where the constraint $C1$ represents bounds on the refractive index of a typical off-the-shelf LC E7 (Merck) [17], [18]. The optimization problem given in (15) is highly non-convex and cannot be approached by traditional optimization algorithms. To that end, a metaheuristic solution method based on the sine-cosine algorithm (SCA) is levaraged to find the suitable refractive index for the optimal data rate performance. The motivation for exploiting the SCA compared to other metaheuristics is its several advantages, such as a straightforward approach, ease of implementation, superior convergence property, and local optima avoidance. The proposed SCA-based solution is detailed in the following subsection.

B. Proposed Solution Approach

The SCA is a population-based metaheuristic introduced in [19] and recently applied in [20]. It solves optimization problems by randomly generating initial candidate solutions and causing them to iteratively shift towards the optimal solution using a sine-cosine-based mathematical model. At the start of the algorithm at iteration t, I search agents, whose positions represent various potential solutions to the problem (15), are randomly deployed within the boundary of the solution space. The fitness of the agents is assessed via the objective function (14), and the fittest agent is designated as the destination point $\mathcal{D}^t$. At the $t+1$-th iteration, each agent updates its solution using

$$s_i^{t+1} = \begin{cases} s_i^t + r_1 \times \sin\left(r_2\right) \times \left|r_3\mathcal{D}^t - s_i^t\right| & \text{if } r_4 < 0.5,\\ s_i^t + r_1 \times \cos\left(r_2\right) \times \left|r_3\mathcal{D}^t - s_i^t\right| & \text{if } r_4 \ge 0.5,\end{cases} \tag{16}$$

where s_i^t represents the solution at t-th iteration for agent i, s_i^{t+1} is the current solution, and $|\cdot|$ denotes an absolute value. The parameters r_1, r_2, r_3, and r_4 take on pseudo-randomly generated numbers that influence the search procedure of the algorithm and the current and best solution positions. More specifically, r_1 denotes the direction of the agents' next movement in the search space and can be obtained as

$$r_1 = a - t\frac{a}{T}, \tag{17}$$

with a and T being a constant value and a predetermined maximum iteration number, respectively. The parameter $r_2 \in [0, 2\pi]$ dictates to what extent the movement should be towards or outwards from the destination point. The parameter $r_3 \in [0, 2]$ controls the influence of the destination point on how far the current solution should be from it. Finally, the parameter $r_4 \in [0, 1]$ equally switches between the sine and cosine search paths as indicated in (16). The fitness of the agents is determined using (14), and the fittest agent so far becomes the new destination point. The algorithm repeats the steps mentioned above until a stopping criterion (e.g., the maximum iteration number or the precision of the global optimal solution) is satisfied. The proposed SCA-based procedure is summarized in Algorithm 1.

Algorithm 1: The Proposed Algorithm for Rate Optimization.

Input: I, T, and a;
Stage one
Set $t = 0$;
Initialize the set of random solutions (i.e., agents) s_i^t, $\forall i$;
Evaluate the fitness of each solution by the objective function (14);
Select the best solution as $\mathcal{D}^t$;
Stage two
Set $t = 1$
while *no convergence* **do**
  Update the parameters r_1, r_2, r_3, and r_4;
  Update the solutions s_i^t, $\forall i$ using (16);
  Check for agents that violate constraint $C1$;
  Update $\mathcal{D}^t$ if there is any better solution;
  Set $t = t + 1$;
end while
Output: $\eta_c^* = s_{i^*}$, where i^* is the agent and η_c^* denotes the global optimum. The external voltage required to obtain η_c^* can be determined from (10) and (11).

C. Computational Complexity Analysis

The computational complexity of the proposed solution mainly depends on the tasks performed in stages one and two. The tasks of generating the initial set of random solutions, evaluating their fitness, and selecting the destination point require $\mathcal{O}(I)$ operations each. Hence, the computational complexity of stage one can be given as $\mathcal{O}(I)$. The computational complexity of the second stage, which involves updating the agents' solution using to (16), evaluating their fitness via (14), and updating $\mathcal{D}^t$ is $\mathcal{O}(IT)$. The overall worst-case computational cost for solving (15) using Algorithm 1 is $\mathcal{O}(I) + \mathcal{O}(IT) \approx \mathcal{O}(IT)$.

TABLE I
SIMULATION PARAMETERS

Parameter	Value	Parameter	Value
η_{e}	1.7	N_o	10^{-21} A^2/Hz
η_{o}	1.5	$T(\varphi)$	1
η_{a}	1.0	φ_{FoV}	85°
v_{th}	1.34 V	f	1.5
v_o	1	q	3
d	0.75 mm	$\phi_{1/2}$	70°
r_{eff}	12 pm/V	R_{PD}	0.53 A/W
B	200 MHz	A_{PD}	1 cm^2

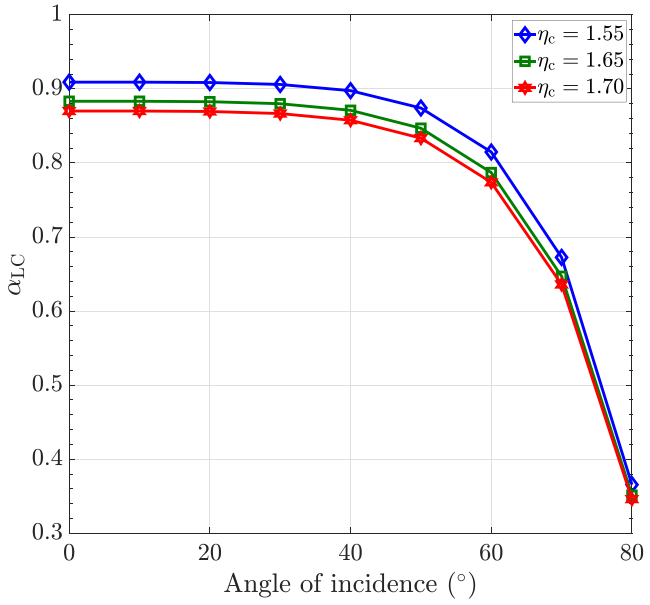

Fig. 2. Transition coefficient versus angle of incidence for LC RIS with different refractive index.

IV. SIMULATION RESULTS

Without loss of generality, a 5 m × 5 m × 3 m room size, a single AP and one user are considered. The AP is deployed at 2.5 m × 2.5 m × 3 m while the position of the user is random and according to a uniform distribution. The values for the parameters I and a are set to 2 and the rest are summarized in Table I.

Fig. 2 shows the influence of the angle of incidence, φ, on the transition coefficient, α_{LC}, of an LC RIS for different values of the refractive index η_{c}. It can be observed that α_{LC} decreases with an increase in η_{c} for any given φ. Moreover, the intensity of the refracted light gradually decreases with an increase in the angle of incidence until $\varphi = 60°$ and then starts decreasing at a steeper rate for increasing values of φ. The reason is that, for values of φ above 60°, the light beams L_1 and L_2 approach the refraction limit and, as a result, a greater proportion of L_1 gets reflected and less amount gets refracted. This figure reveals that α_{LC} is mainly impacted by the angle at which the transmitted light impinges on the LC RIS as well as the value of the refractive index. Since α_{LC} affects the overall channel gain as given in (1), it is important to ensure that φ does not exceed 60° in order to guarantee higher values for α_{LC}.

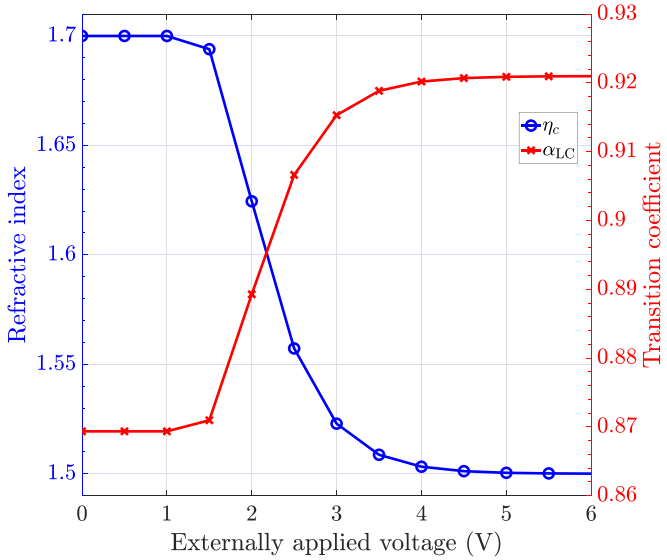

Fig. 3. Refractive index and transition coefficient versus the applied voltage.

Fig. 3 depicts how the refractive index and the transition coefficient of the LC RIS vary with the externally applied voltage, v_e. It can be observed that the value of the refractive index starts decreasing when the applied voltage $v_e > v_{th}$ and saturates when $v_e \geq 5$ V. With regards to the transition coefficient, it starts increasing when $v_e > v_{th}$ and saturates when $v_e \geq 5$ V. These observations can be explained by the fact applying the external voltage induces a change in the molecular orientation (i.e., tilting) of the LC. The tilting of the molecules changes the refractive index in the direction of the tilt and, this in turn, affects the transition coefficient. This figure reveals that as little as up to 5 V is all that is needed to efficiently control the LC RIS as any voltage above 5 V does not yield significant changes.

Fig. 4 illustrates the exponential (e-fold) rate of increase in the intensity of the emerged light from the LC RIS in the presence of an applied voltage. In this figure, the applied voltage is varied from 0 to 5 V since it was revealed in Fig. 3 that voltages outside this range do not affect any properties (e.g., refractive index and transition coefficient) of the LC RIS. For each voltage, the tilt angle and the refractive index can be determined from (11) and (10), respectively. The e-fold gain for that voltage and refractive index can be calculated from (12). It can be seen from this figure that light signals of distinct wavelengths get amplified at different rates when the same voltage is applied. More specifically, for light signals of wavelengths 510 nm, 550 nm, and 670 nm, up to ten, eight, and six-fold gain in the intensity of the emerged light can be obtained from the LC RIS, respectively, for the considered values of the externally applied voltage.

Fig. 5 shows the convergence rate of the proposed algorithm for light signals of different wavelengths. Clearly, Algorithm 1 converges within 20 iterations for all the wavelengths. This highlights its fast convergence rate.

Finally, Fig. 6 compares the data rate performance of the proposed LC RIS-based receiver and optimization algorithm

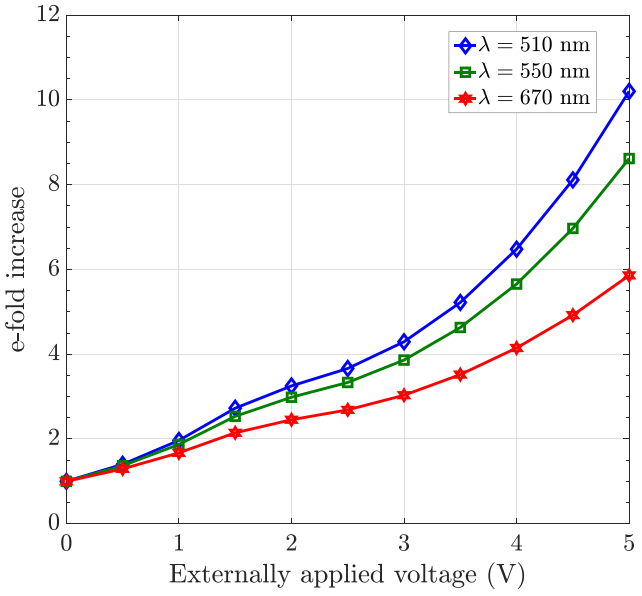

Fig. 4. E-fold increase in the intensity of the emerged light versus the applied voltage.

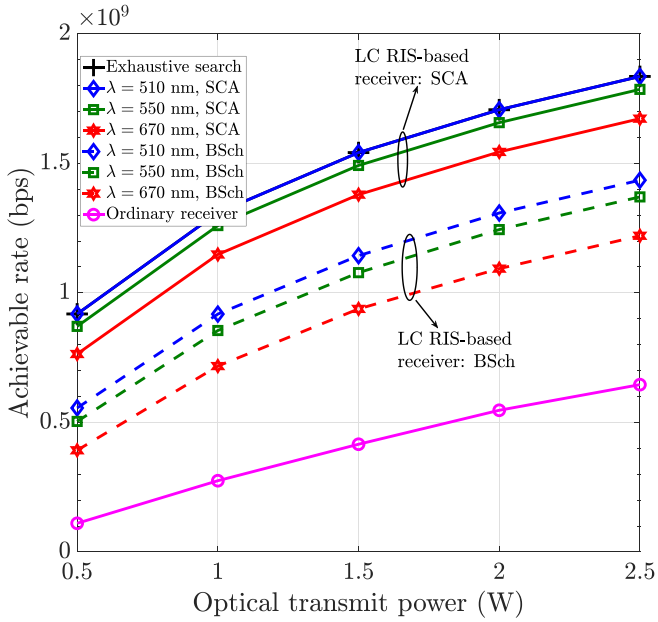

Fig. 6. Achievable data rate versus transmit optical power for light signals of different wavelength: LC RIS-based receiver versus ordinary receiver.

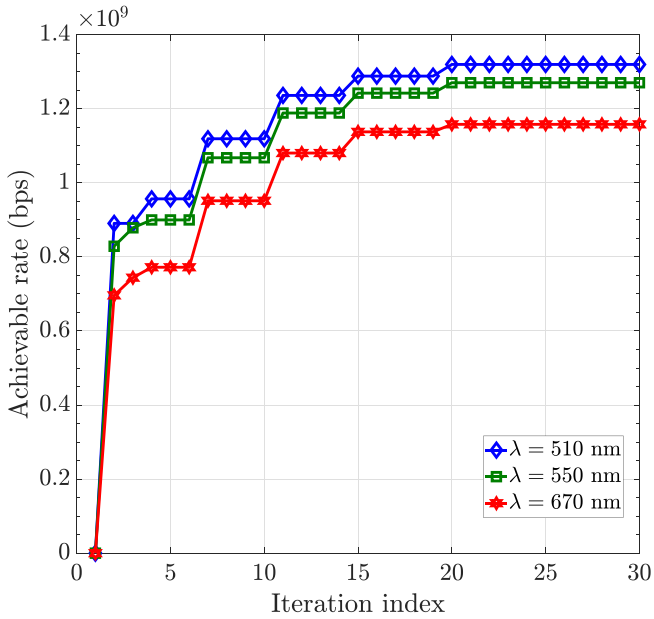

Fig. 5. The convergence rate of Algorithm 1.

with that of (1) an ordinary receiver (i.e., without the LC RIS); (2) a BSch; and (3) the exhaustive search for different transmit power levels. This is done for light signals of different wavelengths since the data rate performance of the LC RIS-based receiver is affected by the wavelength of the transmitted light. The considered BSch involves randomly selecting any feasible value for the refractive index. The curves in this figure are obtained by averaging over 10,000 independent realizations. Several insights can be drawn from this figure. Firstly, it demonstrates that augmenting the transmit power improves the data rate for the LC RIS-based and the ordinary receivers. Secondly, it can be observed that the data rate performance of the proposed SCA scheme matches that of the exhaustive search. Thus, the proposed algorithm can obtain the optimal solution within 20 iterations. Thirdly, the figure reveals that the LC RIS-based receiver with the proposed SCA algorithm can achieve up to 731%, 688%, and 591% improvement in data rate for transmitted light signals of wavelengths 510 nm, 550 nm, and 670 nm, respectively, when compared to that of the ordinary receiver. Moreover, it can be seen from Fig. 6 that the proposed SCA scheme significantly outperforms the BSch for all the considered wavelengths. This demonstrates the effectiveness of the proposed optimization scheme and establishes the LC RIS-based receiver as an efficient way to enhance the data rate performance of VLC systems.

V. Conclusion

In this paper, a novel RIS-based receiver technology for incident light steering and amplification as well as data rate improvement in VLC systems has been presented. The proposed RIS-based receiver uses tunable LCs whose refractive index can be controlled via an externally applied voltage. A channel model characterizing the propagation of the light signals from the AP to the receiver has been proposed. In addition, the principle behind the incident light amplification and the equation for the amplification gain coefficient have been explicitly provided. The main challenge for this novel LC RIS-based receiver design is to determine the value of the refractive index of the LC RIS and the corresponding required external voltage for different user positions. To that end, a non-convex optimization problem for optimizing the refractive index as well as the required voltage

for the LC RIS to guarantee the highest data rate performance has been formulated and a low-complexity solution based on the SCA has been proposed. Simulation results have revealed that the proposed LC RIS-based receiver and the SCA scheme can dramatically improve the data rate performance when compared to baselines such as the random allocation and the ordinary VLC receiver. This paper has revealed that LC RIS-based receivers should be considered a promising solution to satisfying the ultra-high data rate demands in VLC systems without any additional transmit power and bandwidth resources. Interesting future research areas include (i) considering non-LoS communication and user-mobility in VLC systems with mirror array RISs deployed on walls and LC RIS-based receivers, (ii) a practical implementation of the proposed design, (iii) examining the delay and noise performances of the LC-based RIS due to the LC tuning time and photon generation process, respectively.

REFERENCES

[1] M. Noor-A-Rahim et al., "6G for vehicle-to-everything (V2X) communications: Enabling technologies, challenges, and opportunities," *Proc. IEEE*, vol. 110, no. 6, pp. 712–734, Jun. 2022.

[2] X. Wu, M. D. Soltani, L. Zhou, M. Safari, and H. Haas, "Hybrid LiFi and WiFi networks: A survey," *IEEE Commun. Surv. Tuts.*, vol. 23, no. 2, pp. 1398–1420, Apr.–Jun. 2021.

[3] H. Abumarshoud, L. Mohjazi, O. A. Dobre, M. Di Renzo, M. A. Imran, and H. Haas, "LiFi through reconfigurable intelligent surfaces: A new frontier for 6G?," *IEEE Veh. Technol. Mag.*, vol. 17, no. 1, pp. 37–46, Mar. 2022.

[4] S. Aboagye et al., "RIS-assisted visible light communication systems: A tutorial," 2022, *arXiv:2204.07198*.

[5] A. R. Ndjiongue, T. M. N. Ngatched, O. A. Dobre, and H. Haas, "Reconfigurable intelligent surface-based VLC receivers using tunable liquid-crystals: The concept," *J. Lightw. Technol.*, vol. 39, no. 10, pp. 3193–3200, May 2021.

[6] A. R. Ndjiongue, T. M. N. Ngatched, O. A. Dobre, and H. Haas, "Toward the use of re-configurable intelligent surfaces in VLC systems: Beam steering," *IEEE Wireless Commun.*, vol. 28, no. 3, pp. 156–162, Jun. 2021.

[7] G. J. M. Forkel, A. Krohn, and P.A. Hoeher, "Optical interference suppression based on LCD-filtering," *Appl. Sci.*, vol. 9, no. 15, Aug. 2019, Art. no. 3134.

[8] A. Krohn, G. J. M. Forkel, P. A. Hoeher, and S. Pachnicke, "LCD-based optical filtering suitable for non-imaging channel decorrelation in VLC applications," *J. Lightw. Technol.*, vol. 37, no. 23, pp. 5892–5898, Dec. 2019.

[9] A. Krohn, S. Pachnicke, and P. A. Hoeher, "Genetic optimization of liquid crystal matrix based interference suppression for VLC MIMO transmissions," *IEEE Photon. J.*, vol. 14, no. 1, Feb. 2022, Art. no. 7300705.

[10] A. Harlakin, A. Krohn, and P. A. Hoeher, "Liquid crystal display based angle-of-arrival estimation of a single light source," *IEEE Photon. J.*, vol. 14, no. 3, Jun. 2022, Art. no. 6829312.

[11] M. Hébert, R. D. Hersch, and P. Emmel, *Fundamentals of Optics and Radiometry for Color Reproduction*. Wiley, pp. 1–57, Oct. 2014. [Online]. Available: https://onlinelibrary.wiley.com/doi/abs/10.1002/9781118798706.hdi062

[12] B. E. A. Saleh and M. C. Teich, *Fundamentals of Photonics*, 3rd ed. Hoboken, NJ, USA: Wiley, 2020.

[13] W. Demtroder, *Laser Spectroscopy 1: Basic Principles*. Berlin/Heidelberg, Germany: Springer, 2014.

[14] V. Marinova et al., "Photorefractive effect: Principles, materials, and near-infrared holography," in *Wiley Encyclopedia of Electrical and Electronics Engineering.* Hoboken, NJ, USA: Wiley 2016, pp. 1–20.

[15] R. Singh et al., "Dependence of space charge field and gain coefficient on the applied electric field in photorefractive materials," *Opt. Laser Technol.*, vol. 43, no. 1, pp. 95–101, Feb. 2011.

[16] J.-B. Wang, Q. -S. Hu, J. Wang, M. Chen, and J. -Y. Wang, "Tight bounds on channel capacity for dimmable visible light communications," *J. Lightw. Technol.*, vol. 31, no. 23, pp. 3771–3779, Dec. 2013.

[17] J. Beeckman et al., "Non-linear light propagation and bistability in nematic liquid crystals," *Proc. SPIE*, vol. 7414, pp. 86–98, Aug. 2009.

[18] J. Li et al., "Refractive indices of liquid crystals for display applications," *J. Display Technol.*, vol. 1, no. 1, pp. 51–61, Sep. 2005.

[19] S. Mirjalili, "SCA: A sine cosine algorithm for solving optimization problems," *Knowl.-Based Syst.*, vol. 96, pp. 120–133, Mar. 2016.

[20] S. Aboagye, T. M. N. Ngatched, O. A. Dobre, and A. R. Ndjiongue, "Intelligent reflecting surface-aided indoor visible light communication systems," *IEEE Commun. Lett.*, vol. 25, no. 12, pp. 3913–3917, Dec. 2021.